European Journal of Pharmaceutical Sciences 221 (2026) 107510

Contents lists available at ScienceDirect

European Journal of Pharmaceutical Sciences

journal homepage: www.elsevier.com/locate/ejps

In Vitro Investigation of Tapinarof-Loaded Nanogels in an Imiquimod-induced HaCaT–THP-1 Co-Culture Model

Barbara Balogh [a,b,†], Ágnes Klusóczki [a,†], Ágota Pető [a,c], Pálma Fehér [a], Zoltán Ujhelyi [d], Judit Váradi [a], Ildikó Bácskay [a,c,*]

[a] Department of Pharmaceutical Technology, Faculty of Pharmacy, University of Debrecen, Rex Ferenc Utca 1, H-4002 Debrecen, Hungary
[b] Doctoral School of Pharmaceutical Sciences, University of Debrecen, Nagyerdei Körút 98, H-4032 Debrecen, Hungary
[c] Institute of Healthcare Industry, University of Debrecen, Rex Ferenc Utca 1, H-4002 Debrecen, Hungary
[d] Department of Industrial Pharmaceutical Technology, Faculty of Pharmacy, University of Debrecen, Rex Ferenc Utca 1, H-4002 Debrecen, Hungary

A R T I C L E I N F O

Keywords:
tapinarof
inflammation
cytokines
co-culture model
AhR agonist
nanogels

A B S T R A C T

Tapinarof is a novel aryl hydrocarbon receptor (AhR) agonist that has recently been approved for the treatment of psoriasis. Although its clinical efficacy has been proven, in psoriasis, hyperkeratotic plaques and damaged barrier hinder drug penetration from conventional creams and ointments, resulting in poor bioavailability in the deeper layers of the skin. Innovative drug delivery systems can improve targeted action and reduce potential side effects. The primary goal of this study was to evaluate whether tapinarof-loaded nanogels enhance the anti-inflammatory, anti-proliferative, and anti-migratory effects of tapinarof at the cellular level using an *in vitro* HaCaT–THP-1 co-culture model. Initially, experiments were performed using real-time cell analysis (RTCA), and a concentration of 10 μM was found to be the most effective, showing significant cell proliferation inhibition compared to imiquimod and free tapinarof. To demonstrate cell proliferation and migration during inflammatory conditions, a wound healing assay was performed, which showed inhibited cell migration. Subsequently, the levels of inflammatory cytokines (TNF-α, IFN-γ, IL-17A, IL-23) were analyzed by ELISA, which demonstrated that tapinarof incorporated into nanogels reduced cytokine production more effectively than the drug alone. Quantitative PCR (qPCR) analysis confirmed Imiquimod (IMQ)-induced upregulation of *Tnf-α* and *Ifn-γ*, whereas *Il-17a* and *Il-23* did not show measurable transcriptional changes under the experimental conditions. Finally, inhibition of p65 subunit nuclear translocation were observed during NF-κB pathway activation in THP-1 cells by immunofluorescence staining. Overall, our results indicate that nanogel-based delivery systems exhibit enhanced biological effects of tapinarof compared to the free drug in an *in vitro* psoriasis-like co-culture model, highlighting their potential as therapeutic tools for the treatment of various inflammatory skin diseases.

1. Introduction

Tapinarof (3,5-dihydroxy-4-isopropyl-trans-stilbene) is a naturally occurring hydroxylated stilbene produced by bacterial symbionts of entomopathogenic nematodes (Prabath et al., 2022; Silverberg et al., 2024; Smith et al., 2017). In recent years, it has gained considerable attention as a topical therapeutic option for inflammatory skin diseases, particularly psoriasis (Nogueira et al., 2022; Robbins et al., 2019; J. Zhang et al., 2022). Tapinarof 1% cream (Vtama) was approved by the U.S. Food and Drug Administration (FDA) in 2022 for the treatment of plaque psoriasis in adults and has also received approval in China (Nogueira et al., 2022; Prabath et al., 2022; Zhao et al., 2024). While several newly FDA approved psoriasis therapies target intracellular signaling pathways, such as enzyme inhibitors (e.g., PDE4 or TYK2 inhibitors), tapinarof represents a novel class of topical treatment acting via aryl hydrocarbon receptor (AhR) modulation (Nogueira et al., 2022; Ravindran et al., 2025; Roskoski, 2023). Its efficacy has also been studied in the pediatric population ("Tapinarof for the Treatment of

* Correspondence: Tel.: +36-52-411-717 (ext. 58421)
E-mail addresses: balogh.barbara@pharm.unideb.hu (B. Balogh), klusoczki.agnes@pharm.unideb.hu (Á. Klusóczki), peto.agota@pharm.unideb.hu (Á. Pető), feher.palma@pharm.unideb.hu (P. Fehér), ujhelyi.zoltan@pharm.unideb.hu (Z. Ujhelyi), varadi.judit@pharm.unideb.hu (J. Váradi), bacskay.ildiko@pharm.unideb.hu (I. Bácskay).
† These authors contributed equally to this work.

https://doi.org/10.1016/j.ejps.2026.107510
Received 18 January 2026; Received in revised form 27 February 2026; Accepted 16 March 2026
Available online 19 March 2026

Plaque Psoriasis in Pediatric Subjects," 2021) and has also demonstrated clinical efficacy in atopic dermatitis (Paller et al., 2021; Strober et al., 2022).

Psoriasis is a complex, immune-mediated inflammatory skin disorder characterized by abnormal proliferation of epidermal keratinocytes and excessive levels of inflammatory cytokines (Biswasroy et al., 2021; Jurel et al., 2024; Singh and Awasthi, 2023; Sugumaran et al., 2024). The disease is associated with skin barrier dysfunction and pruritus, which significantly impair quality of life and mental health (Balogh et al., 2025; Smith et al., 2017). Several clinical subtypes are described (e.g., guttate, pustular, plaque, erythrodermic, intertriginous), often accompanied by joint and metabolic comorbidities (Ahmad et al., 2022; Aziz Hazari et al., 2023; Sieminska et al., 2024; Yadav et al., 2024). Its pathogenesis is based on a complex interaction of genetic, environmental and immunological factors (Dawe and Di Meglio, 2025; Furue et al., 2019; Makuch et al., 2022; Sugumaran et al., 2024; Zhu et al., 2022). At the center of the pathomechanism is the activation of the IL-23/IL-17 axis, in which TNF-α and IL-23 produced by dendritic cells promote the production of inflammatory cytokines by Th17 cells, such as IL-17, IFN-γ and IL-22 (Cai et al., 2023; Fernández-Gallego et al., 2021; Nogueira et al., 2022; Sieminska et al., 2024; Singh and Awasthi, 2023). These inflammatory mediators stimulate keratinocyte proliferation, chemokine expression and continuous recruitment of leukocytes (Ahmad et al., 2022; Singh and Awasthi, 2023; Smith et al., 2017; Sugumaran et al., 2024). In addition to inflammatory processes, psoriasis is also associated with oxidative stress, epithelial dysfunction and abnormal regulation of the NF-κB signaling pathway, which modulates keratinocyte and immune cell activity (Smith et al., 2017; Sugumaran et al., 2024).

The AhR is a key regulator of skin homeostasis by influencing cytokine production, barrier protein expression and antioxidant activity, making it a prominent clinical target in the treatment of inflammatory skin diseases (Cai et al., 2023; Fernández-Gallego et al., 2021; Jurel et al., 2024; Nogueira et al., 2022). Tapinarof can bind to the AhR and is able to downregulate IL-17A, IL-17F and IL-23 expression. It also enhances skin barrier integrity by upregulating the expression of filaggrin and loricrin and exerts antioxidant effects by activating the AhR-Nrf2 pathway (Jurel et al., 2024; Nogueira et al., 2022; Smith et al., 2017).

Achieving therapeutic efficacy requires not only the anti-inflammatory potential of the active substance, but also its targeted transdermal delivery and appropriate bioavailability. In psoriasis, hyperkeratotic plaques and damaged barrier function inhibit drug release from conventional creams and ointments, resulting in poor bioavailability in the deeper layers of the epidermis (Aziz Hazari et al., 2023; Sugumaran et al., 2024; Zhu et al., 2022). In this context, nanogels represent a very promising delivery system, as they combine the structural stability and high water content of hydrogels with the enhanced penetration and controlled drug release properties of nanocarriers. This is especially advantageous for lipophilic molecules such as tapinarof, since nanogels can improve drug solubility and the penetration through the stratum corneum. Compared to conventional preparations, nanogels could enhance local bioavailability and reduce frequency of application (Aziz Hazari et al., 2023; Gomes et al., 2023; Mascarenhas-Melo et al., 2022; Vasowala et al., 2024). Furthermore, nanogels can reduce local irritation and enhance patient adherence due to their favourable rheological properties and consistency (Balogh et al., 2025; Mascarenhas-Melo et al., 2022)

In our previous work, we have developed tapinarof-loaded nanogels and have confirmed their physical stability, favorable rheological properties, and biocompatibility on HaCaT cell lines (Balogh et al., 2024).

In the present study, we evaluated the functional efficacy of tapinarof-loaded nanogels in comparison to the free drug using a novel imiquimod-induced HaCaT-THP-1 co-culture model, which reliably mimics the inflammatory microenvironment of psoriasis *in vitro*. To validate the true biological benefit of tapinarof nanoformulations, a model system was desired that could effectively reproduce the complex keratinocyte-monocyte interactions of the disease (Váradi et al., 2024). Our primary goal was to demonstrate that nanogel formulations enhance the anti-inflammatory, anti-proliferative, and anti-migratory properties of tapinarof at cellular level. In our experimental plan, we performed an *in vitro* wound healing assay, real-time cell analysis (RTCA), cytokine profiling (ELISA, qPCR) and immune cell staining to functionally evaluate the effects of the different formulations. The aim of our results was to demonstrate that nanogel-based formulations not only serve as stable carriers but also have the potential to meaningfully enhance the biological efficacy of tapinarof *in vitro*, thereby confirming the relevance of nanogels in the topical therapy of psoriasis.

2. Materials and Methods

2.1. Materials

The HaCaT cell line was obtained from Cell Lines Service (CLS, Heidelberg, Germany), and the THP-1 cell line (TIB-202™) was purchased from the American Type Culture Collection (ATCC, Manassas, VA, USA). Cell culture flasks were obtained from Corning (Corning, NY, USA).

All excipients used for nanogel formulation were of pharmaceutical grade. Tapinarof, triacetin, Tween 80, Dulbecco's Modified Eagle's Medium (DMEM), phosphate-buffered saline (PBS), RPMI 1640 Medium, dimethyl sulfoxide (DMSO), Trypan Blue dye and trypsin–EDTA were purchased from Sigma-Aldrich (St. Gallen, Switzerland). Ethanol 96%, glycerin 85%, and oleic acid were obtained from Molar Chemicals Kft. (Budapest, Hungary). Kollisolv, PEG 400 and Kolliphor EL were supplied by BASF (Ludwigshafen, Germany). Carbopol 940 and Carbopol 934 were obtained from B.F. Goodrich Chemical Company (Charlotte, NC, USA), and triethanolamine were purchased from VWR Chemicals. Labrafil M and Transcutol HP were kindly provided by Gattefossé (Lyon, France). Imiquimod was obtained from MedChemExpress via Bio-Kasztel Ltd. (Budapest, Hungary).

Real-time cell proliferation measurements were performed using the xCELLigence Real-Time Cell Analyzer system (Agilent Technologies, Santa Clara, CA, USA). For these experiments, 16-well E-Plates (Lot: 202220725) were used.

For cytokine analysis, ELISA kits were purchased from Invitrogen (Waltham, MA, USA): human TNF-α (Cat. No. KHC3011), IFN-γ (Cat. No. KHC4021), IL-17A (Cat. No. BMS2017), and IL-23 (Cat. No. BMS2023-3). For the *in vitro* wound healing assay, 24-well plate culture inserts (Cat. No. 80242) were obtained from Ibidi (Gräfelfing, Germany).

For qPCR, PrimePCR™ SYBR® Green Assays specific for human TNF-α (Cat. No. qHsaCEP0040184), IFN-γ (Cat. No. qHsaCED0045843), IL-17A (Cat. No. qHsaCID0015941), IL-23A (Cat. No. qHsaCID0021503) and GAPDH (Cat. No. qHsaCED0038674) were used from Bio-Rad.

2.2. Preparation of Tapinarof-Loaded Nanogels

Tapinarof-loaded nanogels were prepared according to the previously published method (Balogh et al., 2024). Both formulations consisted of 1% tapinarof incorporated into self-emulsifying drug delivery systems (SNEDDS). The qualitative and quantitative composition of the SNEDDS systems is summarized in Table 1. SNEDDS I. was a multicomponent surfactant system consisting of labrafil, triacetin, transcutol HP, kolliphor, PEG 400, and tween 80, while SNEDDS II. was based on a more simple surfactant system composed of oleic acid, tween 80, and ethanol. The prepared SNEDDS were subsequently incorporated into Carbopol-based hydrogel matrices to obtain the final nanogels, the detailed composition and ratios of which are presented in Table 2. Nanogel I. contained 33.33% SNEDDS in a Carbopol 940-based hydrogel and glycerin was added as a humectant, while nanogel II. had 50% SNEDDS content in a Carbopol 934 gel matrix. The formulations also

Table 1
Composition of different SNEDDS.

Composition	SNEDDS I.	SNEDDS II.
Labrafil	6%	-
Triacetin	3%	-
Tween 80	5%	8,75%
Transcutol HP	15%	-
Ethanol	5%	26,25%
Kolliphor	5%	-
PEG 400	5%	-
Oleic acid	-	10%
Purified water	56%	55%

Table 2
Composition of the formulated nanogels.

Composition	Nanogel I.	Nanogel-Tap I.	Nanogel II.	Nanogel-Tap II.
Tapinarof	-	1%	-	1%
SNEDDS	33,3%	33,3%	50%	50%
Glycerin	5%	5%	-	-
Purified water	61,2%	61,2%	49,5%	49,5%
Carbopol 940	0,5%	0,5%	-	-
Carbopol 934	-	-	0,5%	0,5%

included triethanolamine as a neutralizing agent.

These preparations were comprehensively characterized in our previous study. They exhibited nanoscale particle size distribution, low polydispersity index, favorable texture and rheology, controlled drug release behavior, and adequate biocompatibility in HaCaT cells, supporting their suitability for *in vitro* biological evaluation (Balogh et al., 2024).

2.3. Cell Co-culture

HaCaT cells can accurately represent human skin as they are human immortalized keratinocytes. They were cultured in calcium-free DMEM medium supplemented with 10% fetal bovine serum (FBS). HaCaT cells were incubated at 37°C in an atmosphere of 5% CO_2. The cell line was maintained by weekly passages in DMEM. In the case of tests, when the cells had completely grown over the well's membrane or near the 100% confluent stage, the experiments were ready to perform.

THP-1 is a human leukemia monocytic cell line, which has been widely used to study monocyte/macrophage functions (Chanput et al., 2014). THP-1 cells were cultured in T-75 flasks in RPMI 1640 containing 10% FBS and 1% penicillin/streptomycin. THP-1 cells were incubated at 37°C in a 95% humidified atmosphere and 5% CO_2. This cell line was maintained by weekly passages in RPMI 1640.

We created a co-culture with HaCaT and THP-1 cells to establish a cell model. The co-culture was grown in calcium-free DMEM medium supplemented with 10% fetal bovine serum (FBS) at 37°C in a 95% humidified atmosphere and 5% CO_2. On the first day, HaCaT cells were seeded. The next day, when they were attached to the surface, THP-1 cells were added to make a co-culture at least for 24 h (Váradi et al., 2024).

During the experiments, a 1:10 THP-1:HaCaT cell ratio was applied to reflect the physiological predominance of keratinocytes within the epidermis while maintaining sufficient immune cell–derived signaling. This ratio has been previously described and validated in HaCaT–THP-1 co-culture systems developed for the investigation of skin sensitization and inflammatory responses (Eskes, 2019; Hennen, 2017).

2.4. Treatment of the Cells

For cell culture experiments, nanogels were diluted with PBS immediately before use to ensure appropriate osmolarity and compatibility with HaCaT and THP-1 cells. Free tapinarof was dissolved in transcutol HP. Preliminary real-time cell analysis (RTCA) was performed to test API (active pharmaceutical ingredient) alone and API-loaded nanogels at concentrations of 0.1, 1, and 10 μM. Based on these results, 10 μM was identified as the most effective concentration and used in all subsequent functional assays, unless otherwise stated.

Imiquimod (IMQ) was dissolved in DMSO and then diluted with PBS to a final concentration of 1 μM, as previously determined by Váradi et al. (2024).

2.5. Real-Time Cell Analysis of HaCaT–THP-1 Co-Culture Treated with Tapinarof-Loaded Nanogels

During the experiment, we applied the most effective concentration of imiquimod as previously determined by Váradi et al (2024). The aim of the test was to determine the optimal concentration of tapinarof-containing nanogels that we could use for further experiments. The effect of the test samples on cell proliferation, both in the presence and absence of imiquimod, was monitored with the help of the xCELLigence Real-Time Cell Analysis (RTCA) system, which enables real-time monitoring of cellular proliferation and viability. The E-plate 16-well plate is coated with gold microelectrodes to measure electrical impedance. 10.000 HaCaT cells/well were seeded for the E-plate. After 6 hours, when cell attachment happened, 1.000 THP-1 cells/well were added to establish a co-culture. The cultures were incubated at 37°C with 5% CO_2. After 24 hours, the cells were treated with serial dilutions (0.1 μM, 1 μM, and 10 μM) of tapinarof, tapinarof-loaded nanogels, and unloaded (blank) nanogels. The culture medium served as a negative control, while IMQ-containing medium was used as a positive control. Cell proliferation was monitored over a period of 96 hours with data acquisition every 30 minutes. Results were expressed as normalized cell index values calculated by the RTCA Software (Váradi et al., 2024).

2.6. In Vitro Wound Healing Assay to Assess Cell Migration

In vitro wound healing assay was performed to evaluate cell proliferation and migration in the co-culture model. A 24-well plate equipped with wound-making inserts (0.5 mm width) was used for creating the scratch. HaCaT cells were seeded into the two compartments of each insert at a density of 280.000 cells/well, thus 140.000 cell/compartments. THP-1 cells were added to the wells at a density of 28.000 cells/well also after 6 hours. DMEM medium was used throughout the treatment period. The co-culture was incubated at 37°C, after 24 hours, the inserts were gently removed to create the scratch area. To preserve the non-adherent THP-1 cells, no washing step (e.g., with PBS) was performed before treatment. Afterward, the cells were treated with 10 μM tapinarof with or without imiquimod, 10 μM tapinarof-loaded nanogels with or without imiquimod, and 10 μM blank nanogels (without active ingredient). The scratch area was observed and photographed at 0, 6, 12, and 24 hours using a light microscope.

The experiment was terminated after 24 hours. The wells were washed with PBS and fixed with fixative solution for 15 minutes at room temperature. After a second PBS wash, the cells were stained with Trypan Blue for 15 minutes at room temperature. Images were captured using a Zeiss Axioscope A1 microscope (Carl Zeiss AG, Germany).

Cell migration rate was determined by quantifying the gap closure over time using the acquired images. The scratch area at final point (24 h) was compared to the initial scratch area (0 h), and the migration rate was calculated as a percentage of gap closure (Váradi et al., 2024).

2.7. Enzyme-Linked Immunosorbent Assay (ELISA) for Cytokine Quantification

ELISA assays were also carried out on the HaCaT–THP-1 co-culture model. For the experiments, a 12-well Transwell system with permeable polycarbonate membranes (0.4 μm pore size) was used. The basal chamber contained 1500 μL of DMEM. HaCaT cells were seeded in the apical chamber at a density of 300.000 cells/well. After 6 hours, THP-1 cells were added to the apical chamber at a density of 30.000 cells/well to create the co-culture. The cultures were incubated for 3 days at 37°C to allow for complete coverage of the membrane The cells were then treated with the following formulations: 10 μM tapinarof in the presence or absence of imiquimod, and 10 μM tapinarof-loaded nanogels with or without imiquimod. Untreated medium was used as a negative control, while 1 μM imiquimod served as a positive control. After 24 hours of treatment, samples were collected from the apical chamber. The concentrations of TNF-α, IFN-γ, IL-17A, and IL-23 were determined in the supernatants according to the instructions of the manufacturer using ELISA kits (Váradi et al., 2024).

2.8. RNA Isolation and RT-qPCR Analysis of Gene Expression

For the qPCR experiment, 500.000 HaCaT cells were plated in 12-well plates per well. After the cells were settled for 6 h at 37°C, 50.000 THP-1 cells were added to each well after incubation in a 5% CO_2 atmosphere. The co-cultures were maintained under the same conditions for 72 h. After three days, cells were treated with 1 μM imiquimod, 10 μM tapinarof-loaded nanogels, 10 μM tapinarof or a combination of these.

After 24 h of treatment, the medium containing the non-adherent THP-1 cells was collected. This cell suspension was centrifuged, the supernatant was eliminated and the cell pellet was washed with PBS. At the same time, adherent HaCaT cells remaining on the plate were also washed with PBS. Then, 1 ml of TRIzol™ reagent (Invitrogen, Cat. No. 15596026) was added directly to each well to lyse the adherent cells. The THP-1 cell pellet was resuspended in TRIzol lysate and the combined samples were transferred to 1.5 ml RNase-free microfuge tubes (Eppendorf, Invitrogen, Cat. No. F23488) for total RNA extraction. Following cell lysis, chloroform was added to the samples for phase separation, and after intensive vortexing, the samples were centrifuged at maximum rpm at 4°C for 15 minutes. The upper phase was carefully removed and mixed with isopropyl alcohol. We centrifuged again on maximum rpm at 4°C for 10 minutes. Then the supernatant was removed and the RNA pellet was washed with 70% ethanol. After repeated centrifugation at maximum rpm at 4°C for 5 minutes, the supernatant was removed and the pellet was dried and finally dissolved in RNase-free water. RNA concentrations were determined using a NanoDrop ND-1000 spectrophotometer (Thermo Fisher Scientific), as well as the quality of the RNA and analyzed with ND-1000 software V3.3.0.

For complementary DNA (cDNA) synthesis, we used a TaqMan reverse transcription reagent kit (Applied Biosystems, USA) according to the manufacturer's instructions.

Gene expression levels of *Tnf-α, Ifn-γ, Il-17a* and *Il-23* were analyzed using PrimePCR™ SYBR® Green Assays according to the manufacturer's instructions. Human GAPDH was used as an endogenous control. Relative gene expression levels were determined by quantitative real-time PCR using the CFX96 Touch Real-Time PCR Detection System (Bio-Rad). The PCR program consisted of the following steps: 2 minutes at 95°C, followed by 40 cycles of 5 seconds at 95°C and 30 seconds at 60°C. All measurements were performed in triplicate. Normalized gene expression was calculated by the ΔΔCt method (Klusóczki et al., 2019).

2.9. Immunofluorescence Analysis of NF-κB p65 Nuclear Translocation in THP-1 Cells

To assess the activation of the NF-κB signaling pathway, nuclear translocation of the p65 subunit was examined by immunofluorescence staining in THP-1 cells. Before seeding, sterile glass coverslips were placed in the wells of a 16-well plate. THP-1 cells were resuspended in RPMI 1640 medium, and 2 μL of 100 ng/mL phorbol 12-myristate 13-acetate (PMA) solution was added to 20 mL of cell suspension to induce differentiation, since PMA treatment promotes the differentiation of THP-1 monocytes into macrophage-like, adherent cells, thereby helping cell fixation and reliable immunofluorescence analysis. Finally, 50.000 cells/well were seeded. The cells were incubated for 30 hours at 37°C in an atmosphere with 5% CO_2. After incubation, the PMA-containing medium was removed and replaced with PMA-free RPMI 1640 medium. The cells were incubated for a further 24 hours under the same conditions. The medium was then eliminated and replaced with fresh RPMI 1640 medium, and cells were started with 10 μM tapinarof-loaded nanogels with 10 μM tapinarof and 10 μM tapinarof itself. After 24 h of treatment, 1 μM imiquimod was added to the medium to induce inflammation and incubated for 1 h. The cells were then washed twice with 500 μl PBS. Fixation was completed with 4% paraformaldehyde (PFA) for 15 min at room temperature. Permeabilization was performed with a 0.1% Triton X-100 solution to facilitate access of antibodies to the nucleus. Non-specific binding was blocked with 5% fetal bovine serum (FBS). The cells were then incubated with Alexa-Fluor 488 conjugated NF-κBp65 (F-6) antibody (Cat. No. sc-8008 AF488) (2 μg/ml) for 1 h and washed three times with PBS. The nuclear staining was performed with a 1:10.000 dilution of nuclear stain for 10 min, followed by removal of the stain and finally two additional PBS washes. Eventually, the glass coverslips were glued to microscope slides.

Fluorescence imaging was visualized using a Zeiss Axioscope A1 fluorescence microscope (Carl Zeiss AG, Jena, Germany) with Zeiss Immersol™ 518F immersion oil (Cat. No. 201006). Image analysis was performed using ZEN 2012 software (v3.8.99.07000, Carl Zeiss Microscopy GmbH, Göttingen, Germany) (Váradi et al., 2024).

2.10. Statistical Analysis

Data were analyzed with GraphPad Prism 10 and presented as means ± SD. Comparison of the groups in ELISA, qPCR and RTCA analysis was performed with one-way ANOVA test. Significant differences in the figures are indicated with asterisks. Differences were regarded as significant when $p < 0.05$. All experiments were performed in triplicate and repeated independently three times.

3. Results

3.1. Real-Time Cell Analysis of HaCaT–THP-1 Co-Culture Treated with Tapinarof-Loaded Nanogels

The potential anti-psoriatic effect of tapinarof and nanogel-based delivery systems was evaluated by real-time cell analysis (RTCA) in co-culture. The IMQ-induced inflammatory environment resulted in increased cell proliferation, as reported in previous literature (Váradi et al., 2024). Tapinarof itself moderately reduced IMQ-induced proliferation, indicating its anti-inflammatory effect (Fig. 1.). As presented in Fig. 2. and 3., nanogel I. and II. did not cause significant cell proliferation, which suggests their biocompatibility. Both of the tapinarof-containing nanogel formulations reduced the cell proliferation index more effectively than the free active ingredient, especially in the presence of IMQ. Tapinarof combined with nanogel formulations moderated IMQ-induced cell proliferation in a dose-dependent manner. According to the results of the experiment, both nanogels significantly reduced IMQ-induced proliferation, but the nanogel II. formulation produced more favorable results. Based on the RTCA results, 10 μM tapinarof and tapinarof-containing nanogels had the most remarkable biological effect, so this concentration was used in subsequent studies.

Additional RTCA figures representing the free drug and the drug-loaded nanogels in the absence of IMQ N are provided in the Supplementary Materials (Fig. S1–S5).

3.2. In Vitro Wound Healing Assay to Assess Cell Migration

Cell migration was assessed using *in vitro* wound healing assay in the co-culture model. Fig. 4. presents that untreated (control) areas

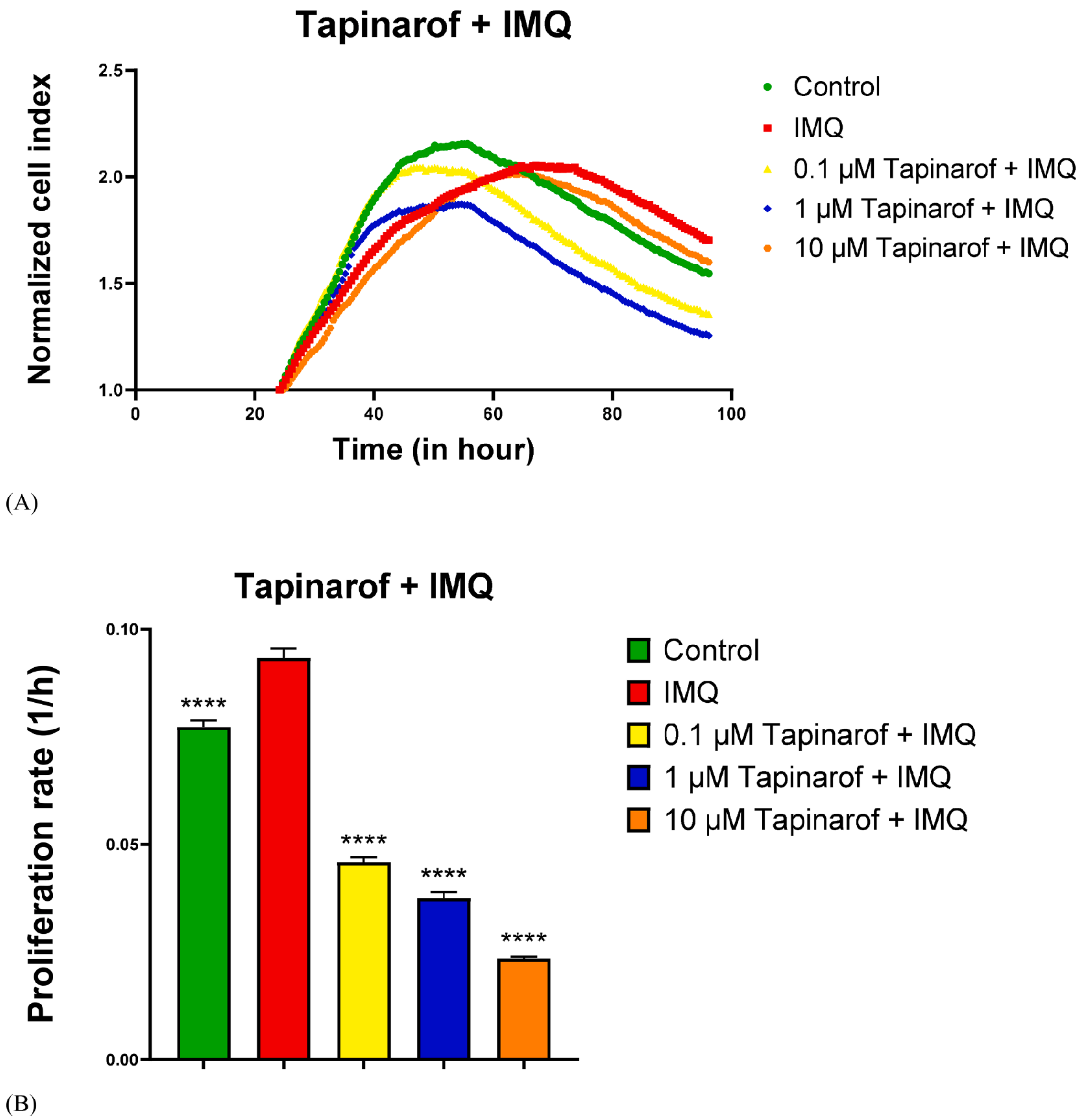

Fig. 1. Investigation of proliferation effect of free tapinarof by Real-Time Cell Analysis (RTCA) (A). The active substance was tested at various concentrations (0.1 µM, 1 µM, and 10 µM) in the presence of IMQ. The initial rate of proliferation was calculated by XCELLigence Software (B). Cell index values were normalized, and curves were monitored for 96 hours. Data are presented as mean ± SDs, n = 3. Each result was compared to the positive control (IMQ). Differences were considered significant at $p < 0.05$; ****$p < 0.0001$.

exhibited cell migration as expected. Complete gap closure was also observed in the IMQ-treated samples, as IMQ enhances keratinocyte proliferation. The treatment of empty nanogels did not affect gap closure, thereby confirming their biocompatibility. Free tapinarof moderately slowed cell proliferation, while API-loaded-nanogel I. also reduced the rate of gap closure in the absence of IMQ. However, a more remarkable anti-migration effect was observed in areas treated with tapinarof-containing nanogel II. formulation. Interestingly, tapinarof, both in its free form and incorporated into nanogels, inhibited cellular gap closure more strongly in an inflammatory microenvironment (in the presence of IMQ) than under physiological conditions. Overall, active substance-loaded nanogel II. proved to be the most pronounced in reducing abnormal keratinocyte migration, thus showing potential in modulating the inflammatory cell response.

Additional representative microscopic images obtained before Trypan Blue staining are included in the Supplementary Materials (Fig. S6).

3.3. Enzyme-Linked Immunosorbent Assay (ELISA) for Cytokine Quantification

Proinflammatory cytokine levels (TNF-α, IFN-γ, IL-17A, and IL-23) were quantified by ELISA in the HaCaT–THP-1 co-culture model. IMQ treatment significantly increased the secretion of all tested cytokines compared to the control group (Fig. 5.), confirming successful induction of the inflammatory response. Tapinarof alone and in nanogel formulations exhibited anti-inflammatory effects. However, nanogel preparations containing API proved to be more effective than the free active ingredient. In the inflammatory microenvironment, free tapinarof moderately reduced IL-23 secretion and indicated no inhibitory effect on other cytokines, in some cases resulting in higher cytokine levels compared to IMQ treatment alone. In the presence of IMQ, tapinarof-loaded nanogel I. reduced TNF-α and IL-23 levels, slightly decreased IL-17A secretion, while no substantial changes were observed in IFN-γ levels. The most potent anti-inflammatory effect was observed with API-loaded nanogel II. treatment, which reduced the levels of all tested

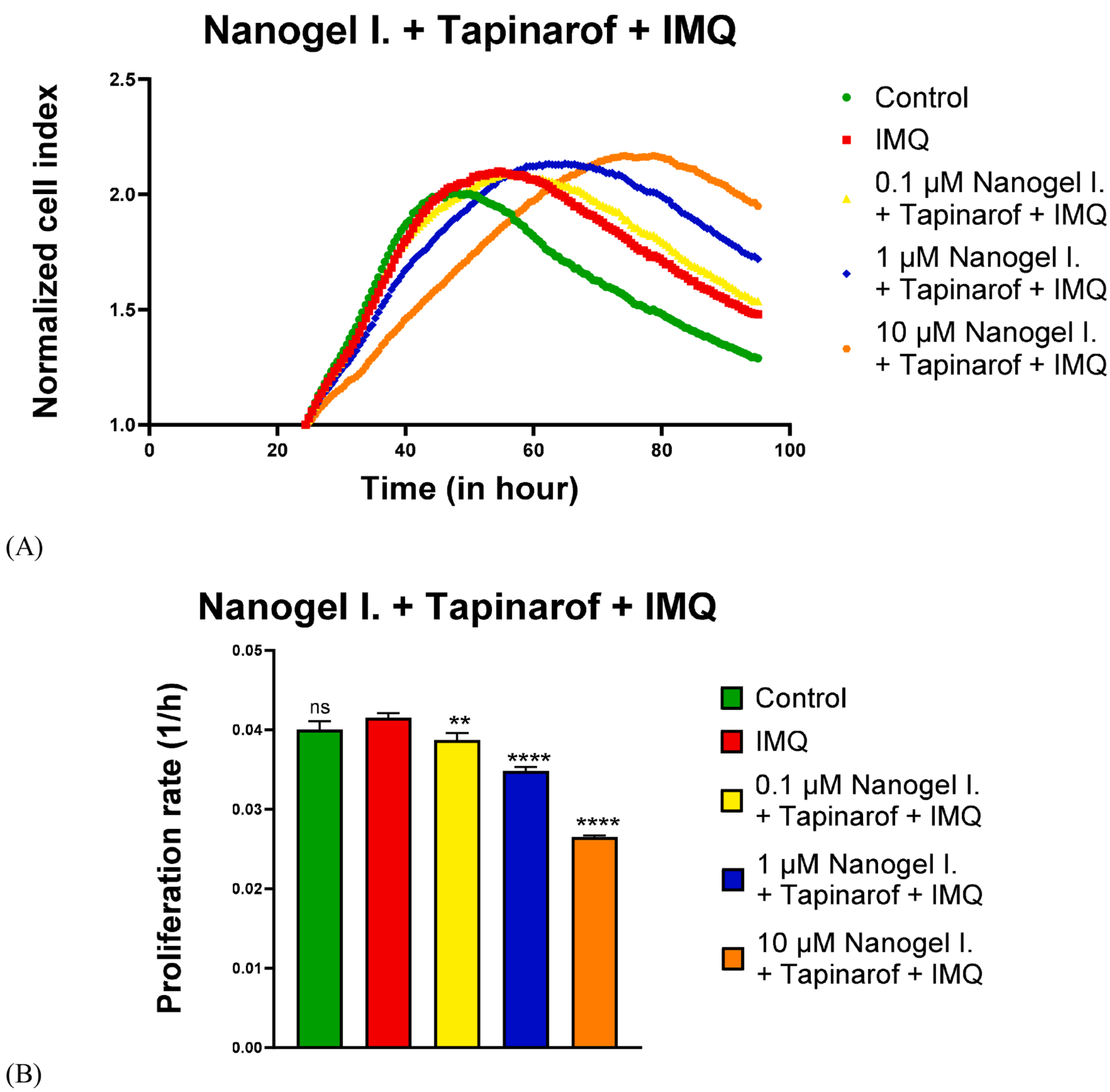

Fig. 2. Investigation of proliferation effect of tapinarof-loaded nanogel I. by Real-Time Cell Analysis (RTCA) (A). The formulations were tested at various tapinarof concentrations (0.1 μM, 1 μM, and 10 μM) in IMQ-stimulated conditions. The initial rate of proliferation was calculated by XCELLigence Software (B). Cell index values were normalized, and curves were monitored for 96 hours. Data are presented as mean ± SDs, n = 3. Each result was compared to the positive control (IMQ). Differences were considered significant at $p < 0.05$; $^{**}p < 0.01$; $^{****}p < 0.0001$ and ns = not significant.

cytokines, including IL-23. Although transcriptional changes in IL-17A and IL-23 were not detectable by qPCR (Fig. 6.), ELISA revealed significant modulation at the protein level. These findings indicate that tapinarof-loaded nanogels effectively decrease IMQ-induced inflammatory cytokine production in this *in vitro* co-culture model.

3.4. RNA Isolation and RT-qPCR Analysis of Gene Expression

The expression of *Tnf-α, Ifn-γ, Il-17a* and *Il-23* genes was determined by qPCR (Fig. 6.). *Tnf-α* gene expression was increased in IMQ-treated samples compared to the control group, confirming successful induction of the inflammatory response. Nanogel I. containing tapinarof produced the most potent anti-inflammatory effect in the presence of IMQ, as it higly attenuated IMQ-induced *Tnf-α* expression. Nanogel II. containing tapinarof and free tapinarof also reduced *Tnf-α* levels, although the effect of nanogel I. proved to be the most effective. *Ifn-γ* gene expression showed a modest increase in response to IMQ stimulation. Treatment with free tapinarof and tapinarof-loaded nanogels resulted in slight decreases in *Ifn-γ* expression in the presence of IMQ. Overall, *Ifn-γ* gene expression remained stable under the experimental conditions. The mRNA expression of *Il-17a* and *Il-23* were below the detection limit in all experimental groups after 24 hours of treatment. Neither IMQ stimulation nor tapinarof or tapinarof-containing nanogels induced measurable transcriptional changes in *Il-17a* or *Il-23* in the HaCaT–THP-1 co-culture model. These findings contrast with the cytokine-level changes observed by ELISA (Fig. 5.), suggesting that cytokine secretion and gene expression were not directly correlated under the applied experimental conditions.

3.5. Immunofluorescence Analysis of NF-κB p65 Nuclear Translocation in THP-1 Cells

The activation of the NF-κB pathway was evaluated by immunofluorescence staining in the THP-1 monocyte cell line by examining the translocation of the p65 subunit into the cell nucleus. As illustrated in Fig. 7., IMQ treatment resulted in p65 nuclear localization, indicating the activation of NF-κB pathway. Free tapinarof treatment resulted in a slight decrease in p65 nuclear translocation, while tapinarof-containing nanogel I showed a moderate inhibitory effect. The most effective IMQ-induced p65 nuclear localization was observed with API-containing nanogel II, indicating a more potent inhibition of NF-κB activation compared to free tapinarof and tapinarof-nanogel I.

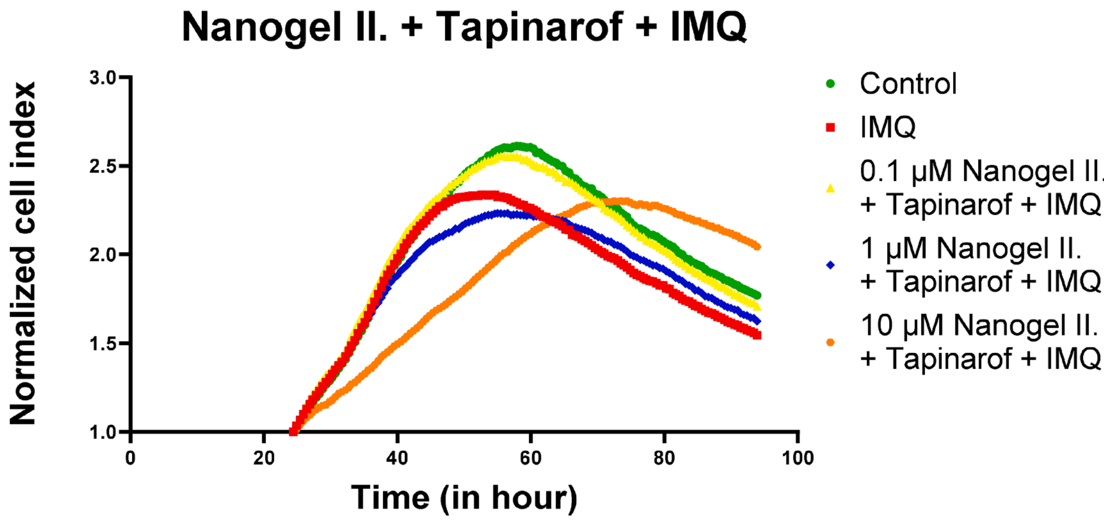

(A)

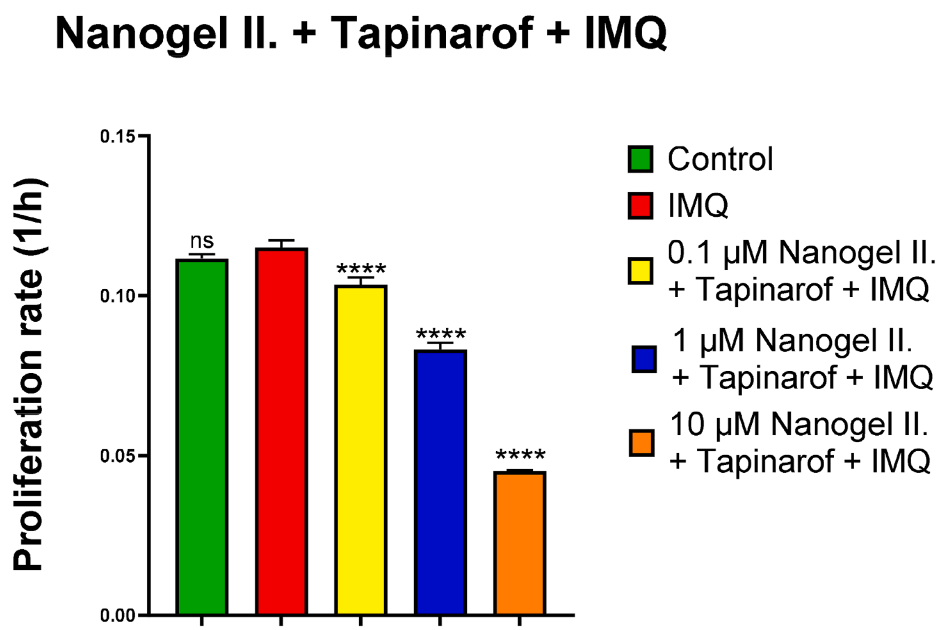

(B)

Fig. 3. Investigation of proliferation effect of tapinarof-loaded nanogel II. by Real-Time Cell Analysis (RTCA) (A). The formulations were tested at various tapinarof concentrations (0.1 μM, 1 μM, and 10 μM) in IMQ-stimulated conditions. The initial rate of proliferation was calculated by XCELLigence Software (B). Cell index values were normalized, and curves were monitored for 96 hours. Data are presented as mean ± SDs, n = 3. Each result was compared to the positive control (IMQ). Differences were considered significant at $p < 0.05$; ****$p < 0.0001$ and ns = not significant.

4. Discussion

In this study, we evaluated tapinarof-containing nanogels based on various parameters using the HaCaT–THP-1 co-culture model. Our results confirmed that tapinarof nanogel preparations are capable of slowing down keratinocyte proliferation, which has already been confirmed in a study on the active ingredient by Cai et al (2023). The cell proliferation inhibitory potential of the nanoformulations was examined using RTCA and *in vitro* wound healing assay. Since there is no scientific data available on the use of RTCA for testing tapinarof, our experiment is of its kind. The measurements were performed with and without the active ingredient, in inflammatory (IMQ-induced) and non-inflammatory environments. Based on the results, both nanogels were able to significantly reduce IMQ-induced proliferation, while the effect of free tapinarof was more moderate. Nanogels without the active ingredient did not enhance cell proliferation. In case of all samples, tapinarof concentration of 10 μM turned out to be the most effective, so we continued further experiments with this dose.

During the *in vitro* wound healing assay, the 10 μM tapinarof concentration resulted in a different migration profile compared to our previous experiment on human dermal fibroblasts, where we tested the active substance at a dose of 40 μM without inflammatory stimuli (Balogh et al., 2024). In the current inflammatory keratinocyte-macrophage model, IMQ increased the cellular gap closure, but treatments containing tapinarof significantly slowed this process. Among the two types of nanogels, nanogel II showed a more favorable tendency than nanogel I. However, in the presence of IMQ, all treatments significantly slowed down the closure of the intercellular gap compared to the free active substance. This suggests a strong antiproliferative and antimigratory effect in the inflammatory cellular environment, which is even more pronounced in the nanogel formulation. This property may be particularly beneficial in pathologies such as psoriasis, which are associated with hyperproliferation and inflammation, and where the goal of therapy is to reduce abnormal keratinocyte

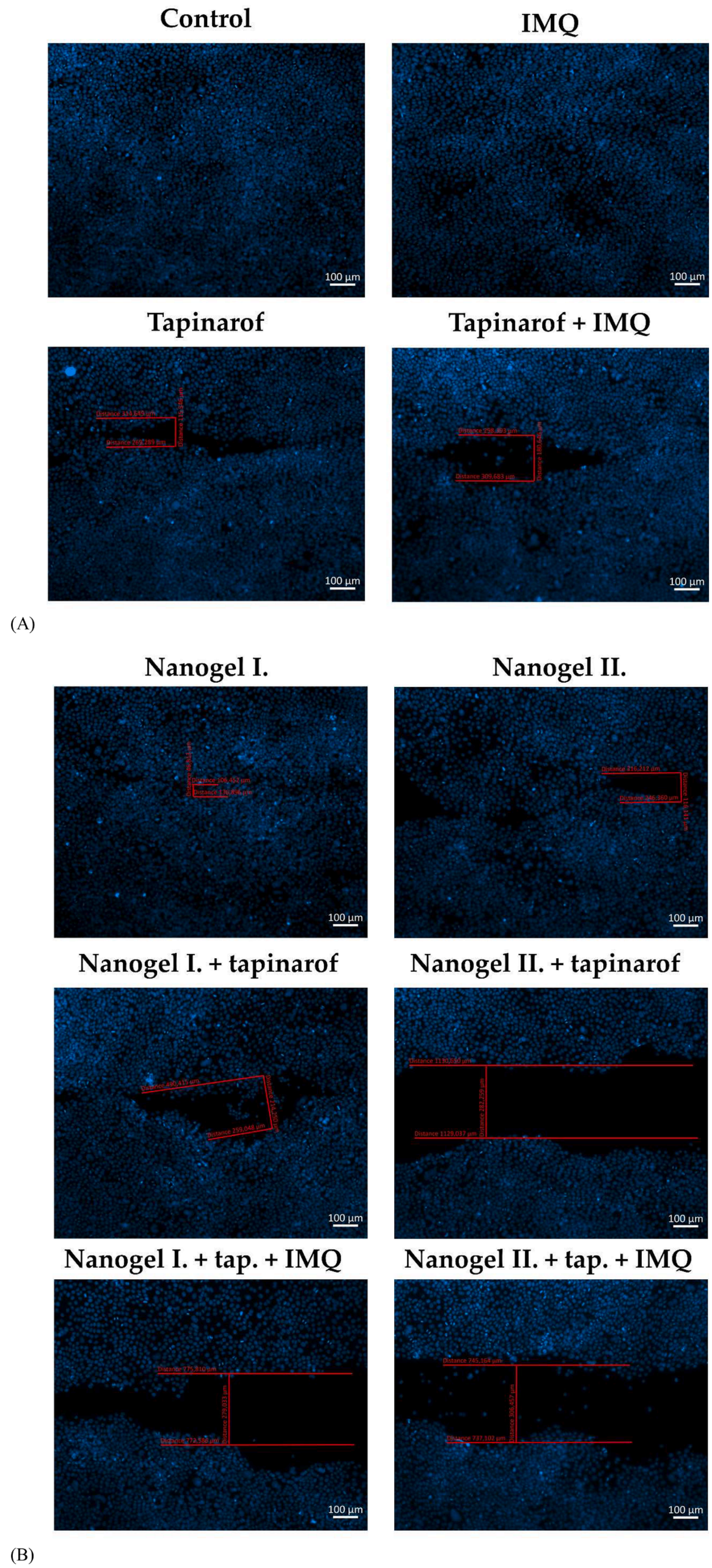

Fig. 4. Representative fluorescence images of gap closure at 24 h post-treatment with tapinarof (A) and its nanogel formulations (B) in the presence or absence of IMQ. Blue: DAPI-stained nuclei. The scratch area is marked in red. Quantification of HaCaT cell migration rate (μm/h) calculated from scratch area measurements at 24 h (C). Data are presented as mean ± SDs, n = 3. Each result was compared to the positive control (IMQ). Statistical analysis was performed using one-way ANOVA, where $p < 0.05$; $***p < 0.001$; $****p < 0.0001$ and ns = not significant. Experiment was performed in triplicate and repeated independently three times.

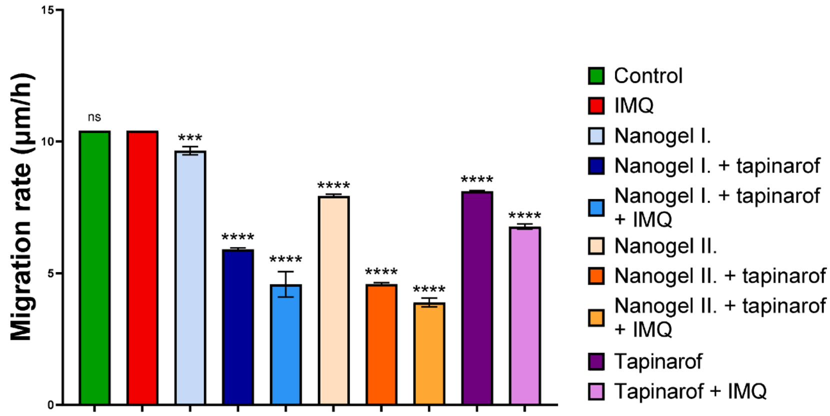

(C)

Fig. 4. (*continued*).

activity.

The ELISA assays were performed to assess the effects of tapinarof-containing nanogel formulations in comparison to free tapinarof on the secretion of key pro-inflammatory cytokines (TNF-α, IFN-γ, IL-17A, and IL-23) in the HaCaT–THP-1 co-culture model. Our results demonstrated that nanogel formulations containing tapinarof resulted in a more pronounced reduction in cytokine secretion compared to the free active ingredient. Nanogel I. reduced TNF-α and IL-23 cytokines and slightly moderated IL-17A secretion under inflammatory conditions, whereas nanogel II. exhibited the most effective anti-inflammatory profile by highly reducing the levels of all four cytokines examined. In contrast, free tapinarof produced only a modest reduction in IL-23 levels and had no detectable inhibitory effect on the other cytokines; in some cases, an increase in cytokine levels was observed in the presence of IMQ.

These findings are generally consistent with previous studies reporting anti-inflammatory effects of tapinarof in different experimental systems. Smith et al. (2017), observed that the API reduced the expression of inflammatory cytokines and improved skin barrier function. Both ELISA and qPCR assays demonstrated a decrease in IL-17A, IL-17F, IL-22, and IL-23 levels, consistent with the anti-inflammatory effect of tapinarof. Similar results were reported by Zhao et al. (2024), who measured a decrease in IL-17 production in dendritic cells treated with tapinarof using ELISA and also observed mRNA expression. In their study, Bissonnette et al. (2021) clearly demonstrated that tapinarof treatment reduced the expression of inflammatory cytokines in skin tissue, including IL-17A, IL-22, IL-23, and IL-1 in a psoriasis mouse model. However, it should be noted that most of these studies were conducted using different biological models, treatment schedules, which may limit direct comparability with the present *in vitro* co-culture model.

In the current study, the qPCR analysis revealed a partial divergence from the ELISA results. Formulations containing tapinarof reduced *Tnf-α* mRNA levels compared to the free drug, while *Ifn-γ* transcription remained largely unchanged in the experimental groups, therefore, no clear tapinarof-mediated effect was detectable in this model. In addition, *Il-17a* and *Il-23* mRNA levels were below the limit of detection in all samples. Correspondingly, no direct conclusion could be drawn between cytokine secretion measured by ELISA and mRNA expression detected by qPCR under the experimental conditions. This discrepancy may reflclet differences in transcriptional and post-transcriptional regulation, as well as temporal variation betweem mRNA expression and protein secretion.

Several studies have already pointed to this phenomenon: the discrepancy between mRNA and protein levels is not exceptional. Protein secretion is influenced not only by transcription, but also mRNA stability, translation, post-translational modifications, and protein degradation. (Vogel and Marcotte, 2012). Another study comparing scRNA-seq (mRNA) and proteome/FACS (protein) data in immune cells also found that the concordance between mRNA and protein levels is not always reliable and that there can be significant discrepancies between the results (Li et al., 2020). Eichelbaum et al. (2014) demonstrated temporal kinetic studies in activated macrophages that the transcriptional responses often peak earlier than the corresponding protein-level changes: the mRNA level peaks rapidly (often within 2–6 hours) and then declines, while the secreted protein accumulates gradually with a delay. Other further studies confirm that mRNA expression is often temporally dissociated from secreted cytokine levels, with mRNA peaks often occurring well before measurable extracellular protein accumulation (Israelsson et al., 2020; Young et al., 2020).

Taken together, the observed divergence between ELISA and qPCR results reflects a known limitation of simplified *in vitro* co-culture systems. Although tapinarof-containing nanogels clearly modulated cytokine secretion in this co-culture model, no definitive conclusions can be drawn regarding transcriptional regulation or the involvement of specific signaling pathways based solely on these data. Nevertheless, the consistent suppression of cytokine release observed by ELISA supports the functional anti-inflammatory potential of tapinarof nanogel formulations in this psoriasis-like *in vitro* model.

The intracellular localization of the NF-κB p65 subunit assessed by immunofluorescence staining also confirmed the anti-inflammatory effect. In the present study, imiquimod treatment induced marked nuclear translocation of p65 in THP-1 monocytes. Free tapinarof slightly attenuated this activation. Compared to the free drug, tapinarof-loaded nanogel I. showed a moderate inhibitory effect, while the more potent blocking effect was achieved by the drug-loaded nanogel II.

Although exact mechanisms responsible for this enhanced effect have not been directly investigated, the observed differences suggest that nanogel-based delivery may improve the availability of tapinarof in cells.

To our knowledge, in the literature few studies have directly examined whether tapinarof inhibits NF-κB p65 nuclear translocation in keratinocytes in inflammatory conditions. Earlier studies have mainly focused on tapinarof-induced cytokine modulation and AhR activation, but no data were available on its direct effect on NF-κB signaling.

A recent study revealed that tapinarof inhibited NF-κB p65 nuclear translocation in HaCaT keratinocytes exposed to particulate matter–induced oxidative stress, potentially via AhR/Nrf2 activation (Lin et al., 2025). Moreover, Brito et al. (2023) also demonstrated in a mouse model that tapinarof treatment reduces the activity of several signaling pathways, including NF-κB, JAK/STAT, ERK/MAPK, and mTOR, and modulates IFN-γ, IL-17/23, and TNF-α-mediated signaling in the skin.

Interestingly, other AhR ligands (e.g., indigo) and structurally related polyphenolic compounds (such as resveratrol) have also been

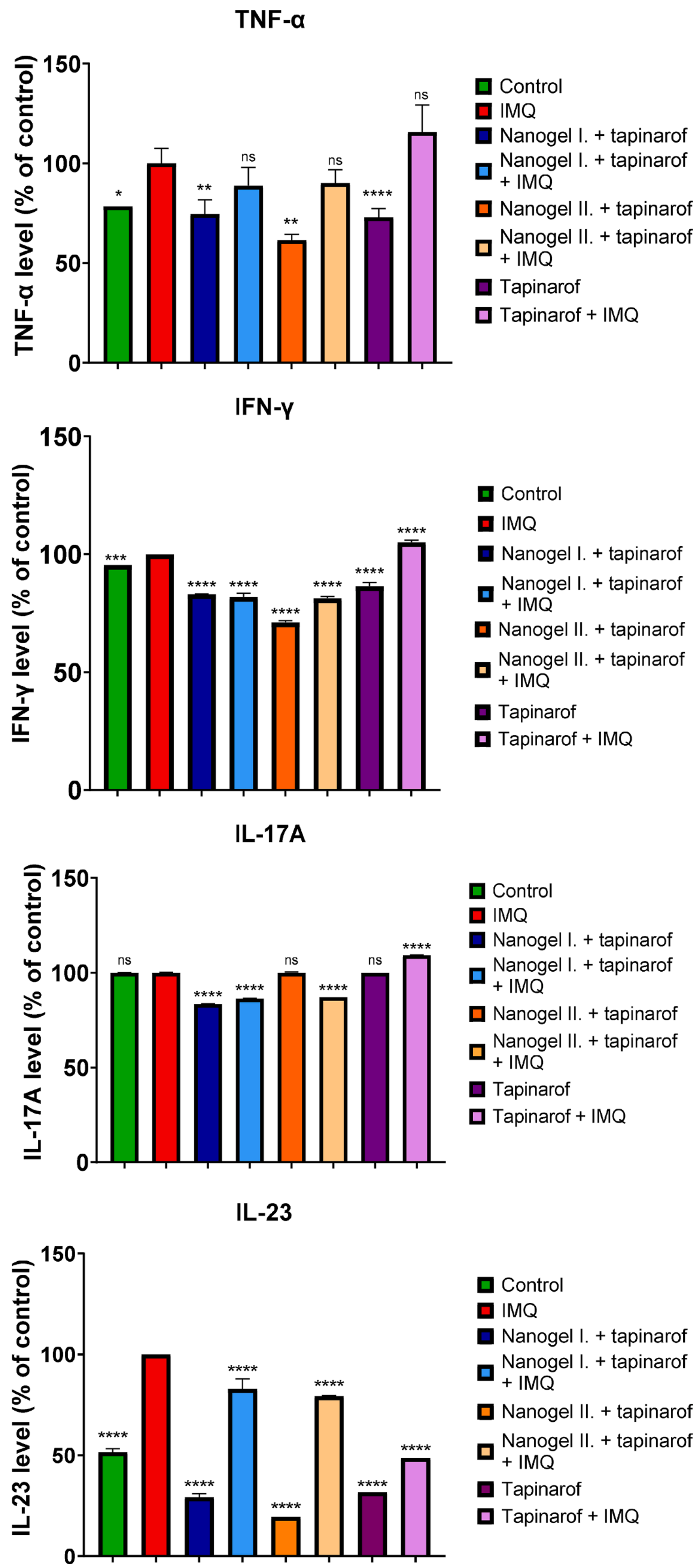

Fig. 5. Levels of pro-inflammatory cytokines in the HaCaT–THP-1 co-culture measured by ELISA after 24 h of treatment. Data are presented as mean ± SDs, n = 3. Each result was compared to and expressed as percentage of the positive control (IMQ). Statistical analysis was performed using one-way ANOVA, where ns = not significant; $p < 0.05$; **$p < 0.01$ and ****$p < 0.0001$.

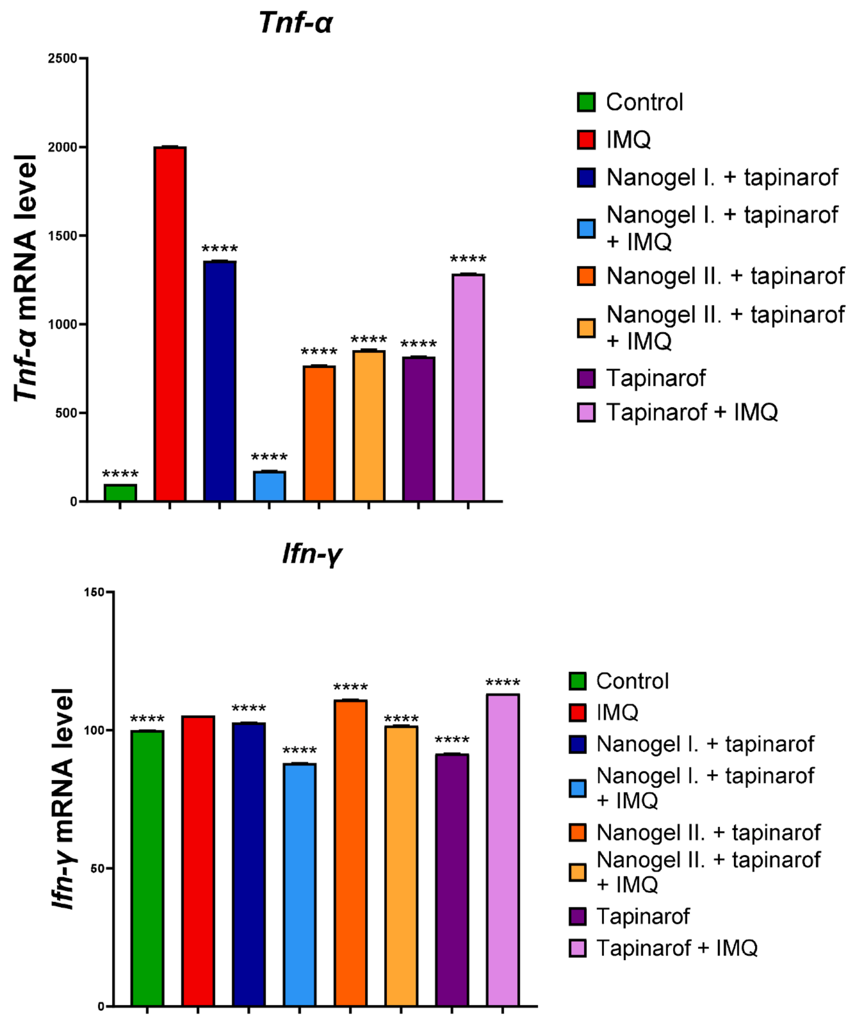

Fig. 6. The mRNA expression levels of *Tnf-α* and *Ifn-γ* cytokines in the HaCaT–THP-1 co-culture treated with different tapinarof formulations (nanogel I. and nanogel II.) in the presence or absence of IMQ. Gene expression levels were normalized to the untreated control (DMEM only). Each result was compared to the positive control (IMQ). Data are presented as mean ± SDs, n = 3. Statistical analysis was performed using one-way ANOVA, where $p < 0.05$ and $^{****}p < 0.0001$.

reported to inhibit NF-κB transcriptional activity. These findings support a broader regulatory interplay between AhR activation and inflammatory signaling pathways (Lin et al., 2024; Pecyna et al., 2020; Rirong Yang et al., 2013).

The presented results suggest that nanogel-based drug delivery can improve the *in vitro* biological efficacy of tapinarof in an imiquimod-stimulated HaCaT–THP-1 co-culture model. Based on several experimental endpoints, tapinarof-containing nanogels were more effective at reducing IMQ-induced inflammatory responses than the free drug.

Notably, formulation-dependent differences were observed between the two preparations. Nanogel II. (with a higher SNEDDS content and lower diversity of surfactants) showed a more pronounced inhibitory effect on NF-κB signaling pathway activation, more effective reduction of inflammatory cytokine secretion in ELISA assays, and more strongly attenuated keratinocyte migration and proliferation in the *in vitro* wound healing and RTCA experiments. In contrast, nanogel I. (with a lower SNEDDS content and higher diversity of surfactants) revealed a more pronounced effect in qPCR-based gene expression assays.

Although the exact molecular mechanisms behind the observed effects cannot be clearly determined based on the current results, several possible explanations can be suggested based on the physical-chemical and biological properties of nanogels. Primarily, it could be the sustained drug release behavior of nanogels that ensures prolonged exposure of cells to drug concentrations. Several reports have been reported on prolonged release profiles related to nanogel systems, and it is known that they enhance pharmacological effects compared to free drugs. In addition, incorporation into a nanogel matrix can protect the active ingredient from physicochemical degradation and improve its solubility, especially in the case of lipophilic molecules like as tapinarof. (Ferozekhan et al., 2024; Manimaran et al., 2023). Increased cellular uptake may also contribute to the observed effects. Thank to their nanoscale size and large surface area, nanogels may promote closer interaction with cell membranes and facilitate the intracellular transport of therapeutic agents (Espuche et al., 2024; Y. Zhang et al., 2022). Moreover, surfactants and SNEDDS themselves can enhance skin penetration and even modulate local inflammatory responses, which may contribute to the differences observed between formulations (Ponto et al., 2021).

Importantly, the accurate molecular mechanisms of the observed effects can not be clearly determined based on the present results, the formulation-dependent differences indicate that the composition and structural characteristics of nanogel systems can considerably influence cellular responses to tapinarof.

Taken together, the incorporation of tapinarof into nanogels may represent a promising formulation strategy for the topical treatment of psoriasis, as it can improve the anti-inflammatory effect of the active ingredient *in vitro*.

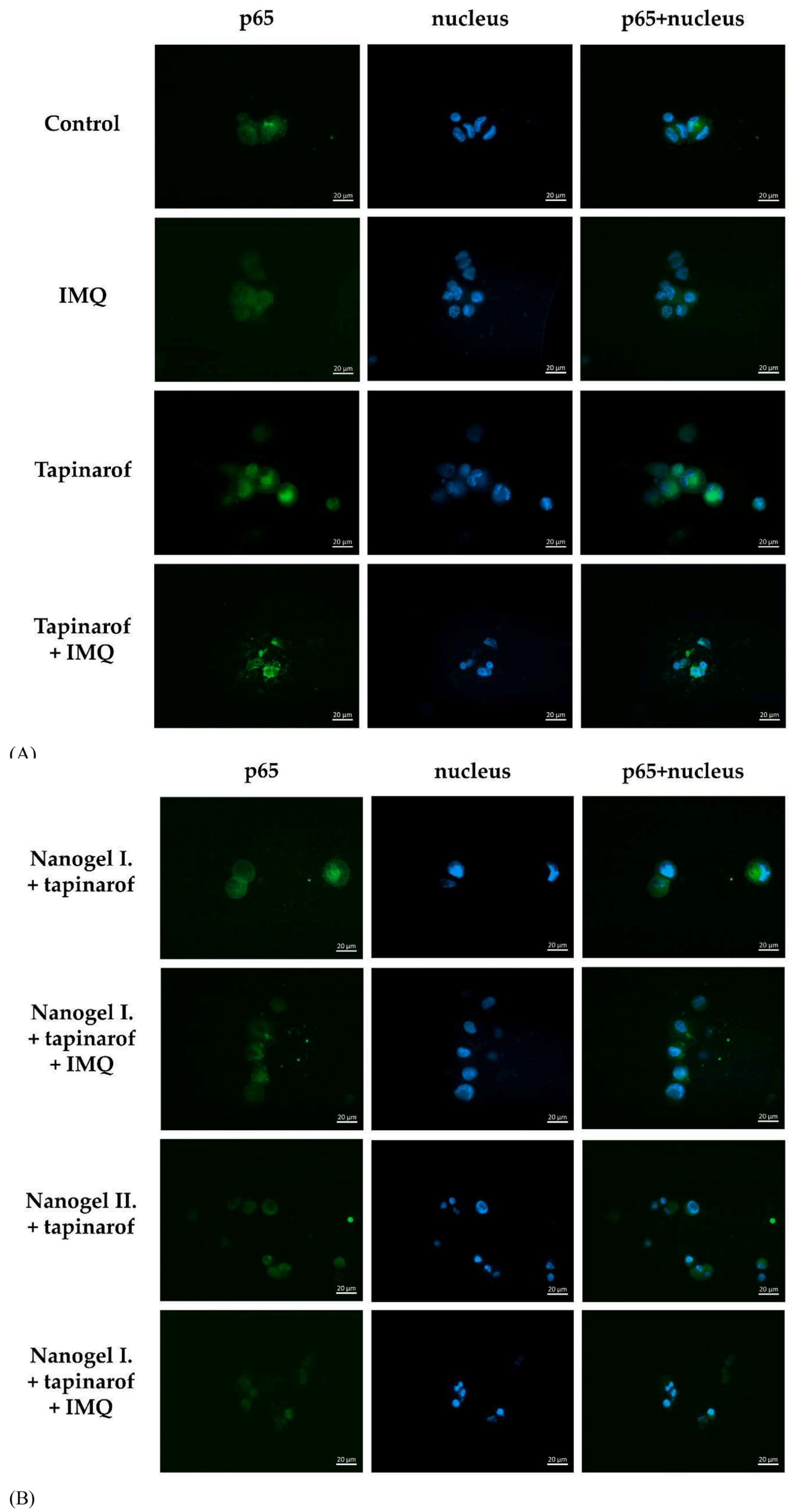

Fig. 7. NF-κB p65 subunit translocation in THP-1 cells upon treatment with tapinarof-containing nanogels. Representative immunofluorescence images showing p65 (green) and DAPI-stained nuclei (blue) in THP-1 cells after 24 h of tapinarof treatment (A) and its nanogel formulations (B). One hour of IMQ incubation was applied. Scale bar = 20 μm. Nucleus/cytosol intensity means the ratio of the fluorescence intensity of NF- κB immunostaining in the cell nuclei and cytoplasm (C). Results are presented as mean ± SD of n = 5. Each result was compared to the positive control (IMQ). Differences were considered significant at $p < 0.05$; $^{**}p < 0.01$ and $^{****}p < 0.0001$.

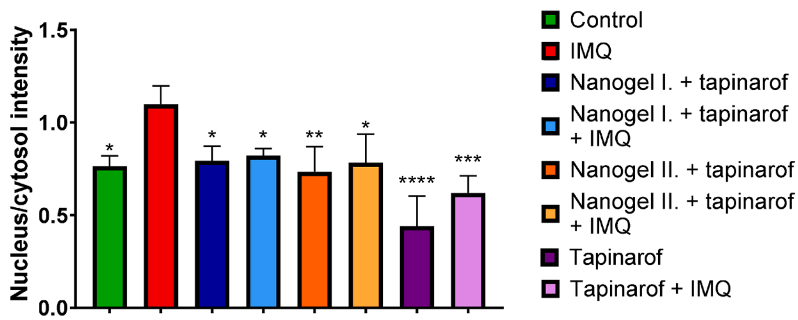

(C)

Fig. 7. (*continued*).

5. Conclusions

Our results show that nanogel-based delivery systems loaded tapinarof enhance the anti-inflammatory and anti-proliferative effects of tapinarof on cells in an imiquimod-induced HaCaT–THP-1 co-culture model. Compared to free drug, nanogel formulations more effectively reduced inflammatory cytokine secretion, inhibited keratinocyte migration and proliferation, and suppressed NF-κB pathway activation in immune cells. These results highlight the potential of nanogel-based delivery systems to improve the biological efficacy of tapinarof at the cellular level. Further studies in more complex biological models are needed to confirm their therapeutic relevance.

Funding

Project no. TKP2021-EGA-18 was implemented with the support provided by the Ministry of Culture and Innovation of Hungary from the National Research, Development and Innovation Fund, financed under the TKP2021-EGA funding scheme and by 2022-1.2.2-TÉT-IPARI-UZ-2022-00006 Common research and development of different prototypes containing natural herb extract for industrial utilisation. The scientific work/research and/or results publicised in this article were achieved with the sponsorship of Gedeon Richter Talentum Foundation in the framework of the Gedeon Richter Excellence PhD Scholarship of Gedeon Richter. Supported by the EKÖP-25-3-II University Research Scholarship Program of the Ministry for Culture and Innovation, from the National Research, Development and Innovation Fund.

Supplementary Materials

Fig. S1. Investigation of proliferation effect of nanogel I. by Real-Time Cell Analysis (RTCA) (A). The formulations were tested at various tapinarof concentrations (0.1 μM, 1 μM, and 10 μM) in the absence of IMQ. The initial rate of proliferation was calculated by XCELLigence Software (B). Cell index values were normalized, and curves were monitored for 96 hours. Each result was compared to the untreated control (DMEM only). Data are presented as mean ± SDs, n = 3. Differences were considered significant at $p < 0.05$; ****$p < 0.0001$ and ns = not significant. **Fig. S2.** Investigation of proliferation effect of nanogel II. by Real-Time Cell Analysis (RTCA) (A). The formulations were tested at various tapinarof concentrations (0.1 μM, 1 μM, and 10 μM) in the absence of IMQ. The initial rate of proliferation was calculated by XCELLigence Software (B). Cell index values were normalized, and curves were monitored for 96 hours. Each result was compared to the untreated control (DMEM only). Data are presented as mean ± SDs, n = 3. Differences were considered significant at $p < 0.05$; ****$p < 0.0001$ and ns = not significant. **Fig. S3.** Investigation of proliferation effect of tapinarof-loaded nanogel I. by Real-Time Cell Analysis (RTCA) (A). The formulations were tested at various tapinarof concentrations (0.1 μM, 1 μM, and 10 μM) in the absence of IMQ. The initial rate of proliferation was calculated by XCELLigence Software (B). Cell index values were normalized, and curves were monitored for 96 hours. Each result was compared to the untreated control (DMEM only). Data are presented as mean ± SDs, n = 3. Differences were considered significant at $p < 0.05$; ****$p < 0.0001$ and ns = not significant. **Fig. S4.** Investigation of proliferation effect of tapinarof-loaded nanogel II. by Real-Time Cell Analysis (RTCA) (A). The formulations were tested at various tapinarof concentrations (0.1 μM, 1 μM, and 10 μM) in the absence of IMQ. The initial rate of proliferation was calculated by XCELLigence Software (B). Cell index values were normalized, and curves were monitored for 96 hours. Each result was compared to the untreated control (DMEM only). Data are presented as mean ± SDs, n = 3. Differences were considered significant at $p < 0.05$ and ****$p < 0.0001$. **Fig. S5.** Investigation of proliferation effect of free tapinarof by Real-Time Cell Analysis (RTCA) (A). The active substance was tested at various concentrations (0.1 μM, 1 μM, and 10 μM) in the absence of IMQ. The initial rate of proliferation was calculated by XCELLigence Software (B). Cell index values were normalized, and curves were monitored for 96 hours. Data are presented as mean ± SDs, n = 3. Each result was compared to the positive control (IMQ). Differences were considered significant at $p < 0.05$; ****$p < 0.0001$. **Fig S6.** Original microscopic images of the degree of closure taken at 0, 6, 12, and 24 hours, showing the migration rate of all treatments performed under inflammatory conditions (A, B). Experiment was performed in triplicate and repeated independently three times.

CRediT authorship contribution statement

Barbara Balogh: Writing – original draft, Methodology, Investigation, Data curation. **Ágnes Klusóczki:** Writing – original draft, Methodology, Investigation, Data curation. **Ágota Pető:** Validation, Methodology, Investigation, Conceptualization. **Pálma Fehér:** Writing – review & editing, Supervision, Formal analysis. **Zoltán Ujhelyi:** Validation, Supervision, Formal analysis. **Judit Váradi:** Validation, Methodology, Formal analysis, Conceptualization. **Ildikó Bácskay:** Writing – review & editing, Validation, Supervision, Resources, Funding acquisition, Conceptualization.

Declaration of competing interest

We wish to confirm that there is no conflict of interest associated with this publication.

Supplementary materials

Supplementary material associated with this article can be found, in the online version, at doi:10.1016/j.ejps.2026.107510.

Data availability

Data will be made available on request.

References

A Phase 3 Study of Tapinarof for the Treatment of Plaque Psoriasis in Pediatric Subjects, 2021.

Ahmad, M.Z., Mohammed, A.A., Algahtani, M.S., Mishra, A., Ahmad, J., 2022. Nanoscale Topical Pharmacotherapy in Management of Psoriasis: Contemporary Research and Scope. J. Funct. Biomater. 14, 19. https://doi.org/10.3390/jfb14010019.

Aziz Hazari, S., Kaur, H., Karwasra, R., Abourehab, M.A.S., Ali Khan, A., Kesharwani, P., 2023. An overview of topical lipid-based and polymer-based nanocarriers for treatment of psoriasis. Int. J. Pharm. 638, 122938. https://doi.org/10.1016/j.ijpharm.2023.122938.

Balogh, B., Pető, Á., Fehér, P., Ujhelyi, Z., Bácskay, I., 2025. Tapinarof Nanogels as a Promising Therapeutic Approach. Pharmaceutics 17, 731. https://doi.org/10.3390/pharmaceutics17060731.

Balogh, B., Pető, Á., Haimhoffer, Á., Sinka, D., Kósa, D., Fehér, P., Ujhelyi, Z., Argenziano, M., Cavalli, R., Bácskay, I., 2024. Formulation and Evaluation of Different Nanogels of Tapinarof for Treatment of Psoriasis. Gels 10, 675. https://doi.org/10.3390/gels10110675.

Bissonnette, R., Stein Gold, L., Rubenstein, D.S., Tallman, A.M., Armstrong, A., 2021. Tapinarof in the treatment of psoriasis: A review of the unique mechanism of action of a novel therapeutic aryl hydrocarbon receptor–modulating agent. J. Am. Acad. Dermatol. 84, 1059–1067. https://doi.org/10.1016/j.jaad.2020.10.085.

Biswasroy, P., Pradhan, D., Kar, B., Ghosh, G., Rath, G., 2021. Recent Advancement in Topical Nanocarriers for the Treatment of Psoriasis. AAPS PharmSciTech 22, 164. https://doi.org/10.1208/s12249-021-02057-z.

Brito, G., Gehad, A., Teague, J., Chen, C., Crisler, W., Gray, L., Kim, I., Clark, R., 2023. 1065 The topical AhR agonist tapinarof has broad in vivo immunosuppressive and immunomodulatory effects in human skin grafted mice. J. Invest. Dermatol. 143, S183. https://doi.org/10.1016/j.jid.2023.03.1077.

Cai, Z., Zeng, Y., Shi, X., Zhang, X., Zhu, H., Wang, W., 2023. Benvitimod inhibits MCM6-meditated proliferation of keratinocytes by regulating the JAK/STAT3 pathway. J. Dermatol. Sci. 109, 71–79. https://doi.org/10.1016/j.jdermsci.2023.01.010.

Chanput, W., Mes, J.J., Wichers, H.J., 2014. THP-1 cell line: An in vitro cell model for immune modulation approach. Int. Immunopharmacol. 23, 37–45. https://doi.org/10.1016/j.intimp.2014.08.002.

Dawe, H.R., Di Meglio, P., 2025. The Aryl Hydrocarbon Receptor (AHR): Peacekeeper of the Skin. Int. J. Mol. Sci. 26, 1618. https://doi.org/10.3390/ijms26041618.

Eichelbaum, K., Krijgsveld, J., 2014. Rapid Temporal Dynamics of Transcription, Protein Synthesis, and Secretion during Macrophage Activation. Mol. Cell. Proteomics 13, 792–810. https://doi.org/10.1074/mcp.M113.030916.

Eskes, C., 2019. The HaCaT/THP-1 Cocultured Activation Test (COCAT) for skin sensitization: a study of intra-lab reproducibility and predictivity. https://doi.org/10.14573/altex.1905031.

Espuche, B., Moya, S.E., Calderón, M., 2024. Nanogels: Smart tools to enlarge the therapeutic window of gene therapy. Int. J. Pharm. 653, 123864. https://doi.org/10.1016/j.ijpharm.2024.123864.

Fernández-Gallego, N., Sánchez-Madrid, F., Cibrian, D., 2021. Role of AHR Ligands in Skin Homeostasis and Cutaneous Inflammation. Cells 10, 3176. https://doi.org/10.3390/cells10113176.

Ferozekhan, F., Umashankar, M.S., Narayanasamy, D., 2024. A Comprehensive Review of Nanogel-Based Drug Delivery Systems. Cureus. https://doi.org/10.7759/cureus.68633.

Furue, M., Hashimoto-Hachiya, A., Tsuji, G., 2019. Aryl Hydrocarbon Receptor in Atopic Dermatitis and Psoriasis. Int. J. Mol. Sci. 20, 5424. https://doi.org/10.3390/ijms20215424.

Gomes, G.S., Frank, L.A., Contri, R.V., Longhi, M.S., Pohlmann, A.R., Guterres, S.S., 2023. Nanotechnology-based alternatives for the topical delivery of immunosuppressive agents in psoriasis. Int. J. Pharm. 631, 122535. https://doi.org/10.1016/j.ijpharm.2022.122535.

Hennen, J., 2017. Keratinocytes improve prediction of sensitization potential and potency of chemicals with THP-1 cells 279–288. https://doi.org/10.14573/altex.1606171.

Israelsson, P., Dehlin, E., Nagaev, I., Lundin, E., Ottander, U., Mincheva-Nilsson, L., 2020. Cytokine mRNA and protein expression by cell cultures of epithelial ovarian cancer—Methodological considerations on the choice of analytical method for cytokine analyses. Am. J. Reprod. Immunol. 84, e13249. https://doi.org/10.1111/aji.13249.

Jurel, P., Bahadur, S., Bajpai, M., 2024. Treatment of chronic plaque psoriasis: An overview on current update. Pharmacol. Res. - Rep. 2, 100004. https://doi.org/10.1016/j.prerep.2024.100004.

Klusóczki, Á., Veréb, Z., Vámos, A., Fischer-Posovszky, P., Wabitsch, M., Bacso, Z., Fésüs, L., Kristóf, E., 2019. Differentiating SGBS adipocytes respond to PPARγ stimulation, irisin and BMP7 by functional browning and beige characteristics. Sci. Rep. 9, 5823. https://doi.org/10.1038/s41598-019-42256-0.

Li, J., Zhang, Y., Yang, C., Rong, R., 2020. Discrepant mRNA and Protein Expression in Immune Cells. Curr. Genomics 21, 560–563. https://doi.org/10.2174/1389202921999200716103758.

Lin, C.-H., Ko, H.-H., Wu, J.-Y., Chang, H.-S., Yen, C.-H., Chiu, C.-C., Chen, Y.-F., 2025. Dual activation of AhR and Nrf2 pathways by the natural stilbenoid tapinarof protects against particulate matter-induced skin barrier dysfunction. Toxicol. Appl. Pharmacol. 505, 117559. https://doi.org/10.1016/j.taap.2025.117559.

Lin, Y., Yang, L., Wang, D., Lei, H., Zhang, Y., Sun, W., Liu, J., 2024. Indigo alleviates psoriasis through the AhR/NF-κB signaling pathway: an *in vitro* and *in vivo* study. PeerJ 12, e18326. https://doi.org/10.7717/peerj.18326.

Makuch, S., Dróżdż, M., Makarec, A., Ziółkowski, P., Woźniak, M., 2022. An Update on Photodynamic Therapy of Psoriasis—Current Strategies and Nanotechnology as a Future Perspective. Int. J. Mol. Sci. 23, 9845. https://doi.org/10.3390/ijms23179845.

Manimaran, V., Nivetha, R.P., Tamilanban, T., Narayanan, J., Vetriselvan, S., Fuloria, N.K., Chinni, S.V., Sekar, M., Fuloria, S., Wong, L.S., Biswas, A., Ramachawolran, G., Selvaraj, S., 2023. Nanogels as novel drug nanocarriers for CNS drug delivery. Front. Mol. Biosci. 10, 1232109. https://doi.org/10.3389/fmolb.2023.1232109.

Mascarenhas-Melo, F., Carvalho, A., Gonçalves, M.B.S., Paiva-Santos, A.C., Veiga, F., 2022. Nanocarriers for the topical treatment of psoriasis - pathophysiology, conventional treatments, nanotechnology, regulatory and toxicology. Eur. J. Pharm. Biopharm. 176, 95–107. https://doi.org/10.1016/j.ejpb.2022.05.012.

Nogueira, S., Rodrigues, M.A., Vender, R., Torres, T., 2022. Tapinarof for the treatment of psoriasis. Dermatol. Ther. 35. https://doi.org/10.1111/dth.15931.

Paller, A.S., Stein Gold, L., Soung, J., Tallman, A.M., Rubenstein, D.S., Gooderham, M., 2021. Efficacy and patient-reported outcomes from a phase 2b, randomized clinical trial of tapinarof cream for the treatment of adolescents and adults with atopic dermatitis. J. Am. Acad. Dermatol. 84, 632–638. https://doi.org/10.1016/j.jaad.2020.05.135.

Pecyna, P., Wargula, J., Murias, M., Kucinska, M., 2020. More Than Resveratrol: New Insights into Stilbene-Based Compounds. Biomolecules 10, 1111. https://doi.org/10.3390/biom10081111.

Ponto, T., Latter, G., Luna, G., Leite-Silva, V.R., Wright, A., Benson, H.A.E., 2021. Novel Self-Nano-Emulsifying Drug Delivery Systems Containing Astaxanthin for Topical Skin Delivery. Pharmaceutics 13, 649. https://doi.org/10.3390/pharmaceutics13050649.

Prabath, I., Subramanian, S., Rani, J., 2022. Tapinarof: A Felicitous Discovery in Psoriasis Treatment. J. Pharmacol. Pharmacother. 13, 222–228. https://doi.org/10.1177/0976500X221130851.

Ravindran, R., Muralidharan, P., Govindarajan, A., 2025. Systematizing PDE4 Inhibition in Psoriasis Treatment: Roflumilast Leads the Way. J. Young Pharm. 17, 13–18. https://doi.org/10.5530/jyp.20251506.

Rirong Yang, R.Y., Zhenghua Ren, Z.R., Lei Wang, L.W., 2013. Resveratrol inhibits NF-kB signaling through suppression of p65 and l B kinase activites. Pharmazie 689–694. https://doi.org/10.1691/ph.2013.2916.

Robbins, K., Bissonnette, R., Maeda-Chubachi, T., Ye, L., Peppers, J., Gallagher, K., Kraus, J.E., 2019. Phase 2, randomized dose-finding study of tapinarof (GSK2894512 cream) for the treatment of plaque psoriasis. J. Am. Acad. Dermatol. 80, 714–721. https://doi.org/10.1016/j.jaad.2018.10.037.

Roskoski, R., 2023. Deucravacitinib is an allosteric TYK2 protein kinase inhibitor FDA-approved for the treatment of psoriasis. Pharmacol. Res. 189, 106642. https://doi.org/10.1016/j.phrs.2022.106642.

Sieminska, I., Pieniawska, M., Grzywa, T.M., 2024. The Immunology of Psoriasis—Current Concepts in Pathogenesis. Clin. Rev. Allergy Immunol. 66, 164–191. https://doi.org/10.1007/s12016-024-08991-7.

Silverberg, J.I., Boguniewicz, M., Quintana, F.J., Clark, R.A., Gross, L., Hirano, I., Tallman, A.M., Brown, P.M., Fredericks, D., Rubenstein, D.S., McHale, K.A., 2024. Tapinarof validates the aryl hydrocarbon receptor as a therapeutic target: A clinical review. J. Allergy Clin. Immunol. 154, 1–10. https://doi.org/10.1016/j.jaci.2023.12.013.

Singh, S., Awasthi, R., 2023. Breakthroughs and bottlenecks of psoriasis therapy: Emerging trends and advances in lipid based nano-drug delivery platforms for dermal and transdermal drug delivery. J. Drug Deliv. Sci. Technol. 84, 104548. https://doi.org/10.1016/j.jddst.2023.104548.

Smith, S.H., Jayawickreme, C., Rickard, D.J., Nicodeme, E., Bui, T., Simmons, C., Coquery, C.M., Neil, J., Pryor, W.M., Mayhew, D., Rajpal, D.K., Creech, K., Furst, S., Lee, J., Wu, D., Rastinejad, F., Willson, T.M., Viviani, F., Morris, D.C., Moore, J.T., Cote-Sierra, J., 2017. Tapinarof Is a Natural AhR Agonist that Resolves Skin Inflammation in Mice and Humans. J. Invest. Dermatol. 137, 2110–2119. https://doi.org/10.1016/j.jid.2017.05.004.

Strober, B., Stein Gold, L., Bissonnette, R., Armstrong, A.W., Kircik, L., Tyring, S.K., Piscitelli, S.C., Brown, P.M., Rubenstein, D.S., Tallman, A.M., Lebwohl, M.G., 2022. One-year safety and efficacy of tapinarof cream for the treatment of plaque psoriasis: Results from the PSOARING 3 trial. J. Am. Acad. Dermatol. 87, 800–806. https://doi.org/10.1016/j.jaad.2022.06.1171.

Sugumaran, D., Yong, A.C.H., Stanslas, J., 2024. Advances in psoriasis research: From pathogenesis to therapeutics. Life Sci 355, 122991. https://doi.org/10.1016/j.lfs.2024.122991.

Váradi, J., Oláh, B., Hosszú, D., Fenyvesi, F., Remenyik, J., Homoki, J., Nagy, B., Fejes, Z., Bácskay, I., Klusóczki, Á., 2024. Development of Imiquimod-induced HaCaT-THP-1 co-culture for modeling of psoriasis. Eur. J. Pharm. Sci. 200, 106846. https://doi.org/10.1016/j.ejps.2024.106846.

Vasowala, T., Gharat, S., Mhase, M., Momin, M., 2024. Advances in hydrogels based cutaneous drug delivery system for management of psoriasis. Eur. Polym. J. 202, 112630. https://doi.org/10.1016/j.eurpolymj.2023.112630.

Vogel, C., Marcotte, E.M., 2012. Insights into the regulation of protein abundance from proteomic and transcriptomic analyses. Nat. Rev. Genet. 13, 227–232. https://doi.org/10.1038/nrg3185.

Yadav, T., Yadav, H., Raizaday, A., Alam, M.S., 2024. The treatment of psoriasis via herbal formulation and nanopolyherbal formulation: A new approach. BioImpacts 15, 30341. https://doi.org/10.34172/bi.30341.https://bi.tbzmed.ac.ir/.

Young, S., Fenn, J., Arriero, E., Lowe, A., Poulin, B., MacColl, A.D.C., Bradley, J.E., 2020. Relationships between immune gene expression and circulating cytokine levels in wild house mice. Ecol. Evol. 10, 13860–13871. https://doi.org/10.1002/ece3.6976.

Zhang, J., Cai, L., Zheng, M., 2022. A novel topical treatment for plaque psoriasis: Benvitimod/tapinarof. J. Am. Acad. Dermatol. 86, e137–e138. https://doi.org/10.1016/j.jaad.2021.10.053.
Zhao, Y., Wu, C., Cai, L., Mu, Z., Liu, X., Zhang, W., Zhang, J., 2024. Tapinarof inhibits psoriatic inflammation through inducing tolerogenic dendritic cells and Foxp3+ Tregs. Chin. Med. J. (Engl.) 137, 2877–2879. https://doi.org/10.1097/CM9.0000000000003260.
Zhu, B., Jing, M., Yu, Q., Ge, X., Yuan, F., Shi, L., 2022. Treatments in psoriasis: from standard pharmacotherapyto nanotechnology therapy. Adv. Dermatol. Allergol. 39, 460–471. https://doi.org/10.5114/ada.2021.108445.